JACS
JOURNAL OF THE AMERICAN CHEMICAL SOCIETY
Communication
pubs.acs.org/JACS

Unconventional, Highly Selective CO_2 Adsorption in Zeolite SSZ-13

Matthew R. Hudson,[†,‡] Wendy L. Queen,[†] Jarad A. Mason,[§] Dustin W. Fickel,[⊥,#] Raul F. Lobo,*[,⊥] and Craig M. Brown*[,†,∥]

[†]Center for Neutron Research, National Institute of Standards and Technology, Gaithersburg, Maryland 20899-6102, United States
[‡]Department of Materials Science and Engineering, University of Maryland, College Park, Maryland 20742-2115, United States
[§]Department of Chemistry, University of California, Berkeley, California 94720, United States
[⊥]Center for Catalytic Science and Technology, Department of Chemical Engineering, University of Delaware, Newark, Delaware 19716, United States
[∥]The Bragg Institute, Australian Nuclear Science and Technology Organisation, PMB1 Menai, NSW, Australia

Supporting Information

ABSTRACT: Low-pressure adsorption of carbon dioxide and nitrogen was studied in both acidic and copper-exchanged forms of SSZ-13, a zeolite containing an 8-ring window. Under ideal conditions for industrial separations of CO_2 from N_2, the ideal adsorbed solution theory selectivity is >70 in each compound. For low gas coverage, the isosteric heat of adsorption for CO_2 was found to be 33.1 and 34.0 kJ/mol for Cu- and H-SSZ-13, respectively. From *in situ* neutron powder diffraction measurements, we ascribe the CO_2 over N_2 selectivity to differences in binding sites for the two gases, where the primary CO_2 binding site is located in the center of the 8-membered-ring pore window. This CO_2 binding mode, which has important implications for use of zeolites in separations, has not been observed before and is rationalized and discussed relative to the high selectivity for CO_2 over N_2 in SSZ-13 and other zeolites containing 8-ring windows.

One of the most pressing issues facing the energy sector is the mitigation of greenhouse gases implicated in global warming through pre- and postcombustion capture applications. Efficient and selective capture of CO_2 from industrial flue gas streams is of particular interest as the current strategy, involving absorption in alkanolamine solutions, suffers a lack of corrosion control and significant energy requirements for regeneration.[1] Typical flue gas streams have low concentrations of CO_2: typical N_2:H_2O:CO_2 ratios of 6.5:1:1 by weight and up to 15% CO_2 by volume at pressures of ∼1 bar.[2] The high gas flow rates make porous materials, such as zeolites, metal−organic frameworks (MOFs), and activated carbons, promising options for future separation/sequestration of CO_2.[3] These framework materials typically exhibit high internal surface areas, allowing them to physically adsorb significant amounts of gas. While adsorption capacity is important, high selectivity and facile regeneration are pertinent properties for postcombustion capture. Many physisorption materials offer moderate to weak flue gas−adsorbent interactions, allowing removal at close to or slightly above room temperature. Additionally, the selectivity of a porous adsorbent can be due to a number of effects such as exclusion due to the size/shape of the pores, adsorbent−adsorbate surface interactions, and varying diffusion rates between different components in a gas mixture. Although increasing in numbers, recent reports of physisorption materials that exhibit a high selectivity for CO_2 over N_2 at ambient pressure and temperature are not common.[3,4]

While gas uptake measurements offer a single view of a specific material's potential for gas storage/separation, comparisons between different analogues can afford further insight into the optimization of properties, such as adsorption capacities, binding energies, and selectivities, that are crucial in the design of new, advanced materials for energy-related applications. Cu-SSZ-13 is unique among copper-exchanged zeolites in that there is only one location for the copper cation in the host framework, simplifying the discussion of cation-exchange effects on uptake and selectivity. Cu-Chabazite-type (CHA) zeolites have shown improved hydrothermal stability over other copper-exchanged zeolites, an important property for postcombustion capture of CO_2 in flue streams with water present.[5] Here, we report an investigation of low-pressure CO_2/N_2 sorption in acidic and copper-exchanged derivatives of zeolite SSZ-13, giving deeper insights into the site-specific adsorption properties obtained utilizing neutron powder diffraction (NPD) combined with *in situ* CO_2 and N_2 adsorption. Gas uptake measurements indicate that the low-pressure CO_2 capacity and the ideal adsorbed solution theory (IAST)[6] selectivity relative to N_2 are not significantly impacted upon exchanging Cu cations into the host SSZ-13 framework. We further determine key structural features of the host framework that result in high uptake and selectivity using NPD.

Langmuir surface areas for Cu- and H-SSZ-13 were determined from 77 K N_2 uptake measurements to be 710 and 764 m^2/g, respectively, with a micropore volume of 0.25 and 0.27 cm^3/g, respectively, agreeing with previously reported values (see Supporting Information (SI)).[5d,7] The CO_2 and N_2 adsorption data for H- and Cu-SSZ-13 are presented in Figure 1. The maximum uptake at 1 bar is lower for the Cu^{2+}-exchanged derivative, 3.75 mmol/g (14.2 wt%), compared to the acidic form, 3.98 mmol/g (14.9 wt%), as expected on a gravimetric basis. In terms of the number of moles of CO_2

Received: November 10, 2011
Published: January 10, 2012

   dx.doi.org/10.1021/ja210580b | J. Am. Chem.Soc. 2012, 134, 1970−1973

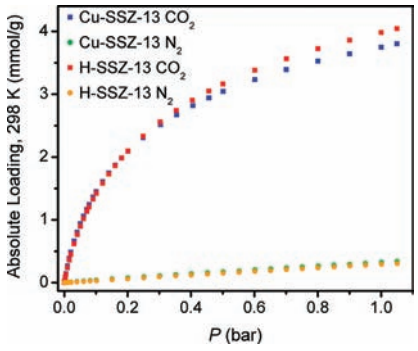

Figure 1. CO_2 (squares) and N_2 (circles) adsorption isotherms for Cu-SSZ-13 (green, blue traces) and H-SSZ-13 (red, orange traces) at 298 K.

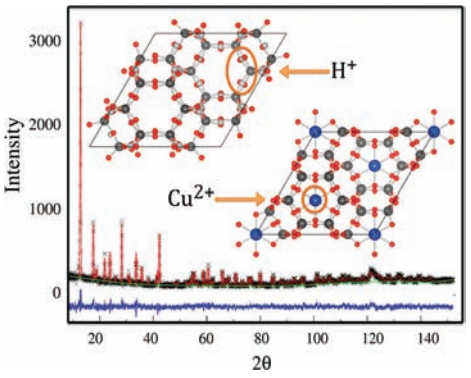

Figure 2. Representative NPD Rietveld refinement of the *in situ* gas-loaded zeolite at a loading of 0.5 CO_2 per Cu^{2+} at 4 K (final goodness-of-fit χ^2 = 1.048). Additional diffraction patterns and structural parameters can be found in the SI.

adsorbed at standard temperature and pressure, H- and Cu-SSZ-13 are in line with the best sorbents for CO_2 uptake and only significantly bested by Mg-MOF-74 (5.4 mmol/g at 0.1 bar).[8] IAST adsorption selectivities for CO_2 over N_2 were calculated for an idealized flue gas mixture of 0.15 bar CO_2 and 0.75 bar N_2 to be 72.0 and 73.6 for Cu- and H-SSZ-13, respectively.

Materials with high overall CO_2 uptake capacity and high selectivity for CO_2 over N_2 generally have high isosteric heats of adsorption ($-Q_{st}$) over a range of surface coverages. This can be a critical parameter, depending on the target separation application. By fitting the adsorption isotherms measured at 298, 308, and 318 K for each material to dual-site Langmuir models (SI), $-Q_{st}$ for CO_2 was determined to average 32.3 and 33.6 kJ/mol (±0.1 kJ/mol) in Cu- and H-SSZ-13, respectively, up to 12 wt% coverage (Figure S4). Since $-Q_{st}$ represents the average binding energy for an adsorbing gas molecule at a specific surface coverage, these almost constant values for $-Q_{st}$ suggest a strong CO_2 binding energy at a single adsorption site or binding at several sites with similar binding energies.

The SSZ-13 zeolites used in this study were determined to have SiO_2/Al_2O_3 = 12, with the copper derivative having Cu^{2+}/Al = 0.35 (SI section S1). SSZ-13 is composed of corner-sharing Al/SiO_4 tetrahedra that form double six-membered-ring cages, which stack in an ABC-type sequence. The cages are further connected to form a cavity with 8-membered windows (consisting of 8 O and 8 Si/Al), ~3.8 Å across, providing size exclusion in the adsorption of gas molecules. Based on potential bond distances and coordination, four sites are suitable for Cu^{2+} to reside. The two most probable coordination sites are "site I", centered between three O(1) atoms at a mean distance of 2.21 Å and found in the center of the 6-ring window, and "site IV", found in the larger 8-membered ring window coordinated to O(2) and O(4) with distances between 2.0 and 2.25 Å. Important for high uptake capacity of SSZ-13 zeolites, site I in the 6-ring window has been determined to be the only copper location through powder X-ray diffraction (XRD).[5d] The high Si/Al ratio results in a low concentration of charge-balancing Cu^{2+} cations, with a site I occupancy of only ~25%. Rietveld refinement of our NPD data obtained on bare Cu-SSZ-13 indicated nuclear scattering density only in the region of site I (Figure 3), with a Cu−O(1) distance of 2.24(1) Å to the three coordinate oxygen atoms and a refined Cu^{2+} occupancy of 0.26(2). This value is lower than the ~0.36 determined by XRD[5d] but agrees well with measured Al content.

NPD data were further collected at sequential, *in situ* loadings of 0.5, 0.75, 1.0, 1.5, and 4.0 CO_2 molecules per Cu^{2+} cation. A representative plot is shown in Figure ; additional diffraction patterns and structural parameters can be found in SI section S3. Fourier difference maps allowed elucidation of CO_2 site positions, and Rietveld refinements provided a final determination of atomic coordinates and CO_2 occupancy as a function of gas loading. At low CO_2 loadings there is preferential occupancy of the gas molecules at a single site (site A, Figure 3), located in the center of the 8-ring window. The CO_2 carbon is centered in the window such that the $O_{ring}-(C)-O_{ring}$ angle is 180°. The closest CO_2−framework interactions include C−O(4), C−O(3), and C−O(2), which are 3.175(4), 3.26(1), and 3.500(6) Å, respectively. The CO_2 molecules, which are canted with respect to the *c*-axis, point toward the center of the small pore and away from the secondary adsorption site (site B) located above the copper cation (Figure 4). The canting angle of the site A CO_2 molecule does not appear to change with increased gas loading. This observation is easily rationalized considering that the canting angle allows the largest possible degree of separation between the CO_2 and framework oxygen atoms, minimizing repulsive interactions between the framework and adsorbate. The O−O distances found between the ring window and CO_2 range from ~3.39 to ~3.82 Å for O(3,4)−O(5) and O(2)−O(5), respectively. The isotropic atomic displacement parameters (ADPs) for CO_2 increase as the occupancy of CO_2 in the window increases (Tables S6−S8), likely indicating some static disorder with higher loadings. Increasing the gas concentration from 0.5 to 1.5 CO_2 per Cu^{2+} increases the concentration of CO_2 in the window but reveals no evidence of nuclear density directly above the Cu^{2+}, indicating that the window is the preferred adsorption site. This window site can accommodate a maximum loading of ~4.5 CO_2 per Cu^{2+} or 12 wt% CO_2. NPD of CO_2 loaded in H-SSZ-13 loaded with 2.0 CO_2 per H^+ (~3.0 CO_2 per Cu^{2+}) also results in CO_2 adsorption at the window site, canted similarly into the pore. This type of CO_2−framework interaction is novel compared to that observed in other zeolites, such as cation-exchanged Y-zeolite,[9] which has end-on CO_2 interacting with the cations, or NaX and H/Na-ZSM-5, where CO_2 molecules form carbonate-like species with framework oxygen atoms.[10]

At the highest loading of 4.0 CO_2 per Cu^{2+}, additional nuclear scattering density is present directly above the metal cation (along the *c*-axis, Figure 4) at site B, revealing end-on CO_2 coordination with a $Cu^{2+}\cdots O{=}C{=}O$ distance of 2.69(3) Å. The ADP of the CO_2 oxygen adjacent to the Cu^{2+} cation is

dx.doi.org/10.1021/ja210580b | J. Am. Chem.Soc. 2012, 134, 1970−1973

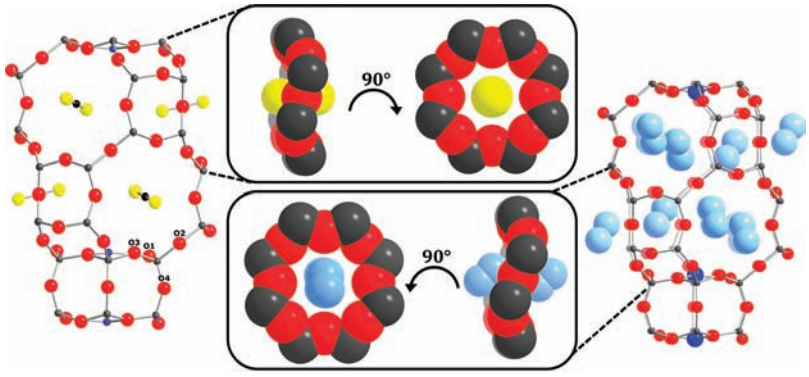

Figure 3. CO_2 adsorption at site A (left, with oxygen labeling scheme) and N_2 adsorption site (right) as determined from NPD measurements of Cu-SSZ-13 at 4 K (yellow spheres, oxygen atoms; black spheres, carbon atoms; pale blue spheres, nitrogen atoms) for one complete CHA cage. The positions of CO_2 and N_2 relative to the 8-ring cage windows are shown as a space-filling representation. It should be noted that the figure represents only the adsorption sites and does not quantify the amounts of gas at each location; the actual occupancy is much greater for CO_2.

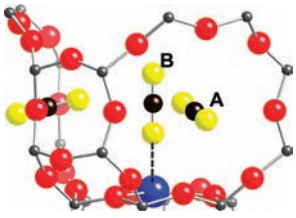

Figure 4. Cut-away view of the CHA cage showing the primary (A) and secondary (B) CO_2 adsorption sites (black, carbons; yellow, oxygens) for the highest CO_2 dosing.

comparable to those of the framework oxygens and site A CO_2 atoms, while the displacement parameters of the remaining site B CO_2 atoms are large. Since NPD data give averaged structural information, and the refined molecular unit is a statistical representation of all site B molecules, the larger ADPs are likely indicative of static disorder or a shallow local potential. To further refine this model, we attempted several other descriptions of the CO_2 units, including refining site B with multiple CO_2 sites that are slightly rotated about the $Cu^{2+}\cdots O$ axis, requiring a highly constrained molecular structure. None of these approaches was satisfactory, and no detailed structural information about the bond distances and angles of the CO_2 can be determined from the data over that of the isotropic ADP model. We postulate that site B disorder is likely the result of competing interactions between the partially occupied CO_2 sites A and B as well as between site B CO_2 and the framework directly around the Cu^{2+}.

To determine specifics of the separation properties, we performed additional *in situ* N_2 diffraction for a loading of 1.5 N_2 per Cu^{2+}. The N_2 is located to the side of the window at an angle of ~128° (O_{ring}–(N_2)–O_{ring}), while the CO_2 is centered (i.e., 180°, Figure 3). The closest N_2–framework interactions are N1–O(3) at ~3.1 Å and N1–O(4) at ~3.5 Å. The N_2 molecules, unlike CO_2 molecules, do not orient perpendicular to the symmetry center of the 8-ring window. The ADPs for N_2 are again large, as with the high loading for CO_2, suggesting there is more disorder in the location of the N_2 outside of the center of the pore window for high N_2 loadings (Table S11). There is no evidence of a secondary N_2–Cu^{2+} adsorption site based on the data with this loading.

The overall high affinity for CO_2 versus N_2 in both forms of the zeolites determined here may stem from several key factors: (1) the small pore size in zeolite SSZ-13 restricts diffusion, (2) the pore window is an ideal diameter for adsorption of CO_2 and unoccupied by cations, and (3) the electrostatic interactions differ between the gases and both the H^+ and Cu^{2+} frameworks. Grand canonical Monte Carlo simulations by Krishna and van Baten considered the selectivity of several 8-ring window zeolite frameworks and suggested that framework flexibility, i.e., lattice dynamics, does not influence the diffusion selectivity in a variety of 8-ring window zeolites, regardless of composition.[11] In SSZ-13, the 3.8 Å pore window is too small for easy diffusion of N_2 (kinetic diameter 3.64 Å), while CO_2 (3.30 Å) can more freely diffuse into the pores. This, coupled with the fact that the framework–CO_2 interaction is the ideal distance for adsorption in the window sites based on van der Waals radii,[12] leads to very high CO_2:N_2 selectivity in SSZ-13. We can calculate the potential energy surface using isolated-molecule DFT calculations for the gas on a central trajectory through the 8-ring window (SI section S4). The minimum energy is found with CO_2 in the center of the window, correlating with the simulations and our NPD data. This is favored by 46.5 kJ/mol compared to any arrangement where CO_2 oxygen atoms are asymmetric with respect to the window.

The energy minima for N_2 on a central trajectory through the 8-ring window are both in the center of the ring and outside the plane of oxygen atoms in the ring with an O_{ring}–(N_2)–O_{ring} angle of 120°. N_2 is favored in the center of the ring by only 8 kJ/mol compared to the side of the window site when on a central trajectory, suggesting there is no energetic reason for locating in the ring as opposed to the side of the window as determined by NPD. Krishna and van Baten also calculated the probability for adsorption at the window site in CHA and found that CO_2 had ~30–40% probability of being located in the pore windows, while N_2 had a <10% likelihood of locating there; they suggested it is the length of the CO_2 molecule that makes this location ideal.[11a] If we consider the difference in quadrupole interactions between framework and CO_2 (quadrupole moment = 13.4×10^{-40} C m^2, polarizability = 26.3×10^{-25} cm^3) and N_2 (quadrupole moment = 4.7×10^{-40} C m^2, polarizability = 17.7×10^{-25} cm^3)[13] over the "length" of the guest molecule, the result is much stronger affinity for CO_2 over N_2 in the window site (SI).

This new-found knowledge of CO_2–framework interaction directly mediated in the center of the 8-ring window may have broad applicability. The quadrupolar interactions should also be valid in the description of other zeolites with high selectivities and 8-ring windows. In the analogous zeolite CHA, albeit at

dx.doi.org/10.1021/ja210580b | J. Am. Chem.Soc. 2012, 134, 1970–1973

differing Si/Al ratios, the CO_2 and N_2 adsorption in the Li-, Na-, and K-exchanged derivatives follows a trend based on the properties of the cations (size and polarizability), with Li-CHA having the highest and K-CHA the lowest CO_2 and N_2 uptakes.[14] It is known that K^+ preferentially locates in the 8-ring window, while Li^+ prefers to exchange into the center of the 6-ring pore.[15] In the case of Na-CHA, Na^+ prefers the 8-ring window site at low and the 6-ring site at high Na^+ content. It is plausible that the availability of window sites in Li- versus Na- and K-CHA can further account for enhanced CO_2 uptake when coupled with the known preference for adsorption at the cation. Diffraction experiments could determine the extent of this effect, if any, with different alkali metal content controlled by varying Si/Al_2 ratios. In the case of 8-ring zeolite NaKA (LTA), the availability of the 8-ring site is even more important. Varying the ratio of Na:K exchanged into the zeolite to optimize selectivity/uptake, Liu et al.[16] determined that at <17 atom% K^+ there is very high CO_2 uptake and selectivity, but at greater K^+ atom% there is a precipitous drop in the CO_2 uptake. There is also a drop in the N_2 uptake above 17 atom% K^+ to essentially no nitrogen uptake. The K^+ in zeolite KA is also found to preferentially occupy the 8-ring window sites.[17]

Through varying the Si/Al ratio, it may be possible to modify the Cu^{2+} content of SSZ-13, further tuning and enhancing the overall uptake *and* separation capacity. Alternatively, CO_2 adsorption may be tuned through chemical substitution of the exchanged cation, allowing manipulation of both charge and polarizability, as demonstrated in the CO_2 uptake of SAPO-34.[18] The most advantageous choice would be to use Cu^+ in place of Cu^{2+}, as a copper-cation-based zeolite should have practical benefits. The use of Cu-SSZ-13 as a separation material is favored since water can significantly impact the overall uptake of the sieving media. This is especially noticeable in the case of the MOF-74 family, where after exposure to humidity, only 16% of the initial uptake capacity is retained in the Mg analogue, one of the leading separation materials based on storage ability.[19] Since water preferentially adsorbs at the copper sites in Cu-zeolites, thereby reducing the uptake capacity at that site,[20] we speculate that Cu-SSZ-13 will not suffer to the same extent from humidity effects that other MOFs and zeolites are subject to since any water should preferentially adsorb at the Cu^{2+} site. From our NPD data, the Cu^{2+} site is responsible for very little of the overall CO_2 uptake ability, making Cu-SSZ-13 an ideal candidate for practical CO_2/N_2 flue-stack separations, where humidity is likely.

■ ASSOCIATED CONTENT

Ⓢ Supporting Information

Experimental details, adsorption isotherms, calculations, NPD refinements, and crystallographic parameters. This material is available free of charge via the Internet at http://pubs.acs.org.

■ AUTHOR INFORMATION

Corresponding Author

craig.brown@nist.gov; lobo@udel.edu

Present Address

[#]SABIC Technology Center−Houston, 1600 Industrial Blvd., Sugar Land, TX 77478-2589

■ ACKNOWLEDGMENTS

R.F.L. and D.W.F. acknowledge financial support from ACS-PRF grant no. 48480-AC5. W.L.Q. gratefully acknowledges the NIST NRC postdoctoral research associateship program. We also thank NSF for providing graduate fellowship support (J.A.M.). We thank V. K. Peterson for providing technical assistance and supplies at ANSTO, and C. J. Kepert for use of the argon glovebox.

■ REFERENCES

(1) Figueroa, J. D.; Fout, T.; Plasynski, S.; McIlvried, H.; Srivastava, R. D. *Int. J. Greenhouse Gas Control* **2008**, *2*, 9. Strazisar, B. R.; Anderson, R. R.; White, C. M. *Energy Fuels* **2003**, *17*, 1034.

(2) Demessence, A.; D'Alessandro, D. M.; Foo, M. L.; Long, J. R. *J. Am. Chem. Soc.* **2009**, *131*, 8784. Powell, C. E.; Qiao, G. G. *J. Membr. Sci.* **2006**, *279*, 1. Granite, E. J.; Pennline, H. W. *Ind. Eng. Chem. Res.* **2002**, *41*, 5470.

(3) An, J.; Fiorella, R. P.; Geib, S. J.; Rosi, N. L. *J. Am. Chem. Soc.* **2009**, *131*, 8401. Millward, A.; Yaghi, O. *J. Am. Chem. Soc.* **2005**, *127*, 17998. Yaghi, O. M.; O'Keeffe, M.; Ockwig, N. W.; Chae, H. K.; Eddaoudi, M.; Kim, J. *Nature* **2003**, *423*, 705.

(4) D'Alessandro, D. M.; Smit, B.; Long, J. R. *Angew. Chem., Int. Ed.* **2010**, *49*, 6058. McDonald, T. M.; D'Alessandro, D. M.; Krishna, R.; Long, J. R. *Chem. Sci.* **2011**, *2*, 2022. Mason, J. A.; Sumida, K.; Herm, Z. R.; Krishna, R.; Long, J. R. *Energy Environ. Sci.* **2011**, *4*, 3030. Sumida, K.; Horike, S.; Kaye, S. S.; Herm, Z. R.; Queen, W. L.; Brown, C. M.; Grandjean, F.; Long, G. J.; Dailly, A.; Long, J. R. *Chem. Sci.* **2010**, *1*, 184. Tan, Y.-X.; Wang, F.; Kang, Y.; Zhang, J. *Chem. Commun.* **2011**, *47*, 770. Chen, S.-S.; Chen, M.; Takamizawa, S.; Chen, M.-S.; Su, Z.; Sun, W.-Y. *Chem. Commun.* **2011**, *47*, 752. Li, J.-R.; Tao, Y.; Yu, Q.; Bu, X.-H.; Sakamoto, H.; Kitagawa, S. *Chem.—Eur. J.* **2008**, *14*, 2771.

(5) (a) Korhonen, S. T.; Fickel, D. W.; Lobo, R. F.; Weckhuysen, B. M.; Beale, A. M. *Chem. Commun.* **2011**, *47*, 800. (b) Kwak, J. H.; Tonkyn, R. G.; Kim, D. H.; Szanyi, J.; Peden, C. H. F. *J. Catal.* **2010**, 1. (c) Bull, I.; Moini, A.; Koermer, G.; Patchett, J. U.S. Patent 7,704,475, 2010. (d) Fickel, D.; Lobo, R. *J. Phys. Chem. C* **2009**, *114*, 1633.

(6) Myers, A. L.; Prausnitz, J. M. *AIChE J.* **1965**, *11*, 121.

(7) Fickel, D. W.; D'Addio, E.; Lauterbach, J. A.; Lobo, R. F. *Appl. Catal., B* **2011**, *102*, 441.

(8) Caskey, S.; Wong-Foy, A.; Matzger, A. *J. Am. Chem. Soc.* **2008**, *130*, 10870. Yazaydın, A.; Snurr, R.; Park, T.; Koh, K.; Liu, J.; LeVan, M.; Benin, A.; Jakubczak, P.; Lanuza, M.; Galloway, D. *J. Am. Chem. Soc.* **2009**, *131*, 18198.

(9) Pirngruber, G. D.; Raybaud, P.; Belmabkout, Y.; Cejka, J.; Zukal, A. *Phys. Chem. Chem. Phys.* **2010**, *12*, 13534.

(10) Martra, G.; Coluccia, S.; Davit, P.; Gianotti, E.; Marchese, L.; Tsuji, H.; Hattori, H. *Res. Chem. Intermed.* **1999**, *25*, 77. Dunne, J. A.; Rao, M.; Sircar, S.; Gorte, R. J.; Myers, A. L. *Langmuir* **1996**, *12*, 5896.

(11) (a) Krishna, R.; van Baten, J. M. *Sep. Purif. Technol.* **2008**, *61*, 414. (b) Krishna, R.; van Baten, J. M. *Microporous Mesoporous Mater.* **2011**, *137*, 83.

(12) Bondi, A. *J. Phys. Chem.* **1964**, *68*, 441.

(13) Bae, Y.-S.; Lee, C.-H. *Carbon* **2005**, *43*, 95.

(14) Ridha, F. N.; Webley, P. A. *Microporous Mesoporous Mater.* **2010**, *132*, 22. Ridha, F. N.; Webley, P. A. *J. Colloid Interface Sci.* **2009**, *337*, 332. Zhang, J.; Singh, R.; Webley, P. A. *Microporous Mesoporous Mater.* **2008**, *111*, 478.

(15) Smith, L. J.; Eckert, H.; Cheetham, A. K. *Chem. Mater.* **2001**, *13*, 385.

(16) Liu, Q.; Mace, A.; Bacsik, Z.; Sun, J.; Laaksonen, A.; Hedin, N. *Chem. Commun.* **2010**, *46*, 4502.

(17) Pichon, C.; Rebours, B.; Paoli, H.; Bataille, T.; Lynch, J. *Mater. Sci. Forum* **2004**, *443−444*, 315.

(18) Zhang, L.; Primera-Pedrozo, J. N.; Hernández-Maldonado, A. J. *J. Phys. Chem. C* **2010**, *114*, 14755. Li, S.; Falconer, J. L.; Noble, R. D. *Microporous Mesoporous Mater.* **2008**, *110*, 310.

(19) Kizzie, A. C.; Wong-Foy, A. G.; Matzger, A. J. *Langmuir* **2011**, *27*, 6368.

(20) Sjövall, H.; Blint, R.; Olsson, L. *J. Phys. Chem. C* **2009**, *113*, 1393.